Bacterial strategies for chemotaxis response

Antonio Celani and Massimo Vergassola[1]

Institut Pasteur, Genomes and Genetics Department, Unit "Physics of Biological Systems," Centre National de la Recherche Scientifique Unité de Recherche Associée 2171, F-75015 Paris, France

Edited by Howard C. Berg, Harvard University, Cambridge, MA, and approved December 8, 2009 (received for review August 26, 2009)

Regular environmental conditions allow for the evolution of specifically adapted responses, whereas complex environments usually lead to conflicting requirements upon the organism's response. A relevant instance of these issues is bacterial chemotaxis, where the evolutionary and functional reasons for the experimentally observed response to chemoattractants remain a riddle. Sensing and motility requirements are in fact optimized by different responses, which strongly depend on the chemoattractant environmental profiles. It is not clear then how those conflicting requirements quantitatively combine and compromise in shaping the chemotaxis response. Here we show that the experimental bacterial response corresponds to the maximin strategy that ensures the highest minimum uptake of chemoattractants for *any* profile of concentration. We show that the maximin response is the unique one that always outcompetes motile but nonchemotactic bacteria. The maximin strategy is adapted to the variable environments experienced by bacteria, and we explicitly show its emergence in simulations of bacterial populations in a chemostat. Finally, we recast the contrast of evolution in regular vs. complex environments in terms of minimax vs. maximin game-theoretical strategies. Our results are generally relevant to biological optimization principles and provide a systematic possibility to get around the need to know precisely the statistics of environmental fluctuations.

biological optimization | *E. coli* | evolution | game theory | strategy

Response networks of living organisms are selected for fast and reliable adaptation to environmental conditions. If the environment is regular, evolution of the response will be driven by the conditions typically experienced by the organism. Examples for microorganisms are long-term memory and the anticipation of environmental changes presented in refs. 1 and 2. For irregular environmental fluctuations, organisms will try to sense the environment and respond by adapting their state. However, if fluctuations are rapid compared to the response time of the organism, it might be more fit to give up on sensing and behave stochastically (3, 4). An alternative source of problems stems from the diversity of the fluctuations. If only two states of the environment are present, two specifically adapted responses are easily evolved and molecularly encoded. This encoding is not possible, though, if the environment is too complex: Conflicts arise then because responses well-adapted to some environmental conditions typically turn out to perform poorly in others. Which response is then evolved by the organism? How sensitive is the evolved response to the precise statistics of environmental fluctuations?

Our scope here is to address the previous questions for bacterial chemotaxis, one of the best characterized systems of response (5). In the absence of chemoattractants, the bacterium *Escherichia coli* is propelled by counterclockwise rotation of its curled flagella at velocities $u \simeq 20$ μm/s for runs whose duration is Poisson distributed with mean value $\tau_r \simeq 1$ s in standard conditions (6). Clockwise rotation of flagella induces tumbling of the bacteria for periods of about 0.1 s (7). Tumblings lead to reorientations of the running direction that make the bacterial motion indistinguishable from a random walk on time scales of a few run/tumble events. In the presence of chemoattractants, the duration of the runs is modulated by the chemotactic pathway (8). The signaling pathway involves processes of (de)phosphorylation that transduce the signal from chemoreceptors down to the flagellar motors. The adaptation pathway involves (de)methylation processes that control the sensitivity of chemoreceptors, which is regulated to match the level of chemoattractant experienced in the recent past (9, 10). Detailed models of the chemotactic pathway are discussed in refs. 11–16, and swimming of synthetic bacteria is simulated in ref. 17. The net response of *E. coli* upon the binding of chemoattractants to the chemoreceptors is to shift the rate of transition between clockwise and counterclockwise rotation of the flagellar motors. When adapted, the bacterium will respond linearly to chemoattractant concentrations eliciting receptor occupancies below their saturation level. Namely, the chemotactic response $K(t)$ is defined as the bias in the fraction of time spent by a flagellum rotating counterclockwise (CCW) vs. clockwise (CW) at time t after a pulse of chemoattractant. The rate of switching from the running mode (CCW) to the tumbling mode (CW) reads

$$\omega_{\mathrm{CCW}\to\mathrm{CW}}(t) = \frac{1}{\tau_r}\left[1 - \int^t K(t-s)c(s)ds\right], \qquad [1]$$

where τ_r is the running time in the absence of chemoattractants and the integral term controls the bacterial response to the time history $c(s)$ of chemoattractant detections. The chemotactic response $K(t)$ of *E. coli* to aspartate (18) is shown in Fig. 1, as obtained by the classical tethering assay (19). The experimental curve is averaged over several cells, yet its shape is typical of the bacterial populations. In particular, a generic property of the curve in Fig. 1 is the fact that the two lobes have equal areas, that is, the integral of the function $K(t)$ is very close to zero. Note that the response to any signal of moderate intensity is obtained via Eq. **1** from the chemotactic response $K(t)$, which explains its fundamental importance.

Questions previously raised for the general case find a specific formulation for chemotaxis: What are the functional and evolutionary forces shaping the response in Fig. 1? Is the shape reflecting a typical property of chemoattractant profiles experienced by the bacterium? If not, are there conflicting evolutionary pressures on the chemotactic response? Why is the integral of the response function in Fig. 1 so close to zero? Information and previous works (20–23) relevant to those issues are briefly summarized hereafter.

As for the environmental conditions where chemotaxis is selected, bacterial motility peaks at specific space-time phases of biofilm development (24) and colony growth, namely, at the entry into the stationary phase (25–27). Nutrients (and cues to locate them) are then running short and the surrounding colony is dense; e.g., the interbacterial distance in figure 1 of ref. 27 is comparable to the bacterial running length. Conditions are harsh and chemoattractant profiles are far from static, with bacteria in

Author contributions: A.C. and M.V. designed research, performed research, analyzed data, and wrote the paper.

The authors declare no conflict of interest.

This article is a PNAS Direct Submission.

[1]To whom correspondence should be addressed. E-mail: massimo.vergassola@pasteur.fr.

This article contains supporting information online at www.pnas.org/cgi/content/full/0909673107/DCSupplemental.

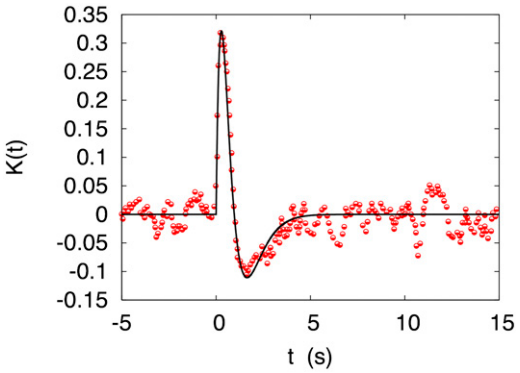

Fig. 1. The experimental chemotactic response $K(t)$ to aspartate (circles) as obtained by measuring the bias (with vs. without chemoattractants) of the fraction of time that a flagellum rotates counterclockwise (18). Bacteria are tethered to a glass slide and subject to a pulse of chemoattractant at $t = 0$. The average of the signal prior to the stimulus defines the zero level on the y axis. The positive and the negative lobes of the response have approximately equal area, which is the property of major interest here. The solid line is our prediction [**10**] of the maximin strategy that allows bacteria to maximize their minimum uptake of chemoattractant in *any* concentration profile thereof. The curve shown here corresponds to a value of the bacterium rotational diffusivity $D = 0.26$ rad^2/s, which is that of a rotation ellipsoid of axes 1 and 0.25 μm, in water at room temperature and is also compatible (see final section of *SI Text*) with measurements of the angular deviations in the tracking of bacterial trajectories (6).

the colony vying for scarce nutrients (and orienting cues) that are available. It is expected that surrounding bacteria will strongly affect the environmental conditions, i.e., the chemoattractant profiles. For *E. coli* in the wild, outside the human gut, it is likely that nutrients and chemical cues will be scarce and come in intermittent patches subject to strong space-time fluctuations. In short, it is unlikely that conditions of strong selection for chemotaxis be characterized by regular profiles of chemoattractants.

The standard explanation for the zero integral of the response function in Fig. 1 is that filtering out the low-frequency (namely, the constant) part of c permits an efficient sensing of its gradients, irrespective of the background level. This feature is positive, yet advantages and disadvantages should be gauged considering both the sensing and the motility aspects of chemotaxis: "Green pastures" (5) should be sensed, but, most importantly for the bacterium, their location should also be reached rapidly and effectively. Because *E. coli* must run to measure variations in the concentrations (28), sensing and motility are entangled, as illustrated quantitatively by the relation [**1**]. Compatibility/conflicts between the requirements of the two functions should then be analyzed jointly. In fact, as first remarked by de Gennes (21), the current of bacteria in the direction of a gradient of chemoattractant is maximized by a positive, single-lobe response $K(t)$: A negative lobe reduces the bacterial drift upgradient. In other words, the sensing of gradients of chemoattractant and their climbing impose conflicting requirements upon the bacterial chemotactic response. A concrete example of a single-lobe response is provided by thermotaxis at 40°: High temperature is a strong repellent and the *E. coli* response is entirely negative so as to descend the gradients of temperature as fast as possible (29). Additional conflicting requirements were remarked in ref. 22: At the stationary state, $\int K(t) = 0$ is far from optimal for the localization of bacteria at high concentrations of chemoattractant, which is optimized by a single-lobe response $K(t)$.

In summary, sensing and motility requirements upon the chemotaxis response are generally incompatible: The widest sensing range has a cost in terms of motility performances. A satisfactory understanding of the response must then consider both advantages and disadvantages, weighting them in terms of bacterial fitness and their quantitative dependency on the environment. This goal is met here, developing the theoretical approach that yields the prediction shown in Fig. 1, in excellent agreement with the experiments. Our approach reverses the scheme in refs. 21 and 22: Rather than the best choices of $K(t)$ and τ_r in particular profiles, we consider all possible chemoattractant profiles for a given $K(t)$ and τ_r. The latter appears more appropriate to the variable conditions experienced by chemotactic bacteria, and additional motivation, as well as a strong connection with game theory, will be established later. Specifically, for a given bacterial $K(t)$ and τ_r, we compute the bacterial uptake of chemoattractant in a generic space-time profile $c(\boldsymbol{x}, t)$. We demonstrate in the next section that the uptake of chemoattractant is a quadratic form, defined by the coefficients $a[c]$ and $b[c]$ in Eqs. **8** and **9**. The eigenvectors corresponding to the lowest eigenvalue of the uptake quadratic form define the profiles of chemoattractant where the given $K(t)$ and τ_r perform the worst (least uptake). Each $K(t)$ and τ_r is thus associated to a certain minimum eigenvalue of the corresponding uptake quadratic form; looking for those $K(t)$ and τ_r such that their minimum eigenvalue is the largest (maximin strategy) yields the prediction in Fig. 1. Finally, in the section preceding *Conclusions*, we analyze the evolution of the chemotactic response for a bacterial population in a chemostat at low-dilution rates, when harsh realistic conditions are obtained. We demonstrate by numerical simulations and analytical arguments that the bacterial response maximizing the minimum uptake indeed emerges from the evolutionary dynamics, providing further support for the relevance of the maximin strategy to bacterial chemotaxis.

Theory for the Bacterial Uptake of Chemoattractant

The analytical calculation for the bacterial chemoattractant uptake as a function of the response function $K(t)$ and running time τ_r involves the following four steps.

First, the response function $K(t)$ is written in the form

$$K(t) = \lambda e^{-\lambda t} \sum_k \beta_k (\lambda t)^k. \qquad [2]$$

The parameter λ^{-1} controls the rescaling of the time variable, whereas the β_ks specify the amplitude and the shape of $K(t)$. Eq. **2** is quite general because it is just a reorganization of the expansion in Laguerre orthogonal polynomials: It follows that any parameterization of the function $K(t)$ (including those with multiple time scales as in ref. 30) can be recast in the form [**2**]. The advantage of Eq. **2** is that the truncation at a finite order in k leaves us with a Markovian dynamics in a space enlarged to include a set of "internal variables." Internal variables store the memory of past detections, and their role is qualitatively analogous to that of the concentration of molecules transducing the signal in detailed models of the chemotactic network. Specifically, let us define internal variables as

$$m_k(t) = \int_{-\infty}^{t} e^{-\lambda(t-t')} (t-t')^k c(X_{t'}, t') dt', \qquad [3]$$

where X_t is the position of the bacterium at time t. The internal variables obey a chain of ordinary differential equations $\dot{m}_k = -\lambda m_k + k m_{k-1}$ for $k \geq 1$, and the equation for $k = 0$ provides the coupling with the chemoattractant signal $\dot{m}_0 = -\lambda m_0 + c(\boldsymbol{X}_t, t)$. If we now truncate at a finite order, the equation for m_k involves only m_k itself and lower orders so that we have a closed set of equations for the m_ks. The lowest-order truncation of the expansion [**2**] that turns out to accurately describe the experimental kernel $K(t)$ features two terms ($k = 1, 2$). We are thus left with three parameters: β_1, β_2, and λ. This reduced setup is the one that we shall consider for simplicity in what follows. Higher-order terms can be treated by the same methods, as we demonstrate in *Higher-Order Parameterization of the Response Function* of *SI Text* showing how the maximin prediction for $K(t)$ is (slightly) modified when higher-order terms are taken into account. Final-

ly, the parameterization [2] of the response and the methods described shortly are of general interest for the input-output relations of response networks, their advantage being that the memory of the system is modeled by preserving the Markov property of the dynamics enlarged to the internal variables.

Second, the previous Markov property enables us to derive a Fokker–Planck equation for the probability density $P(\boldsymbol{x},t,\hat{\boldsymbol{u}},\boldsymbol{m})$ to have the bacterium at position $\boldsymbol{x}$ at time t, running in the direction $\hat{\boldsymbol{u}}$ and with the internal variables having the values $\boldsymbol{m}$:

$$\partial_t P + u\nabla\cdot(\hat{\boldsymbol{u}}P) + \mathscr{M}P = D\nabla^2_{\hat{\boldsymbol{u}}}P - \frac{1-Q}{\tau_r}\left[P - \int W(\hat{\boldsymbol{u}}\cdot\hat{\boldsymbol{u}}')P(\hat{\boldsymbol{u}}')d\hat{\boldsymbol{u}}'\right]. \quad [4]$$

Here, $\mathscr{M}P \equiv \sum_{k=0}\partial_{m_k}[(\delta_{k,0}c(x,t) + km_{k-1} - \lambda m_k)P]$ accounts for the dynamics of the internal variables, D is the rotational diffusivity that perturbs the course of the bacterium, and $\nabla^2_{\hat{\boldsymbol{u}}}$ is the angular Laplacian. The last term of the second line in Eq. **4** accounts for the effects of tumblings. The average run time in the absence of chemoattractant is denoted τ_r. The variable $Q = \sum_{k=1}\lambda^{k+1}\beta_k m_k$ denotes the integral term in Eq. **1** for the expression of $K(t)$ in Eq. **2**. We recall that $Q = \int K(t-s)c(s)ds$ is supposed to be small with respect to unity, i.e., the amplitude of the response matches that of the input signal, e.g., by any mechanism of desensitization. Remark that rescaling the amplitude of the response does not necessarily imply $\int K(t) = 0$. If the latter condition holds, the amplitude of $K(t)$ can ideally be adapted to the rapid part of a signal $c = c_0 + c'$ featuring a slow and a rapid (comparable to τ_r) component. Conversely, if $\int K(t) \neq 0$, the condition $Q \ll 1$ forces the amplitude of $K(t)$ to scale with the slowly varying background component c_0 (usually larger than the fluctuations) with the consequence that only fluctuations of sufficient amplitude could be effectively detected. As it was already mentioned, this feature is less convenient for sensing, yet it can be advantageous for motility, and responding only to gradients of sufficient amplitude is not a priori senseless. In practice, the amplitude of K is left as a free parameter in the linear theory hereafter (see *Response Saturation and Adaptation* of *SI Text* for nonlinear effects). In Eq. **4**, we have assumed for simplicity that the bacterium responds to the concentration, not to noisy measurements thereof (see *Noisy Response* in *SI Text* for the general case). We have also neglected the duration of tumbling events, but formulas for a finite tumbling time can be found in *Finite Tumbling Time* of *SI Text*. The transition probability for the changes of direction $\hat{\boldsymbol{u}}' \to \hat{\boldsymbol{u}}$ during the tumbling phase is denoted $W(\hat{\boldsymbol{u}}\cdot\hat{\boldsymbol{u}}')$. A priori, the function W could be subject to optimization, and we show in *SI Text* that using different Ws correlated with the tumbling's duration can indeed be an advantageous strategy. This modulation is plausible mechanistically because the longer the bacterium tumbles, the more decorrelated the input and output directions can be. These effects will be interesting to analyze in more detail but are expected to be weaker than those considered here. We take then $W = (1 + \hat{\boldsymbol{u}}\cdot\hat{\boldsymbol{u}}')/4\pi$, i.e., the experimental distribution of turning angles (6), featuring a preference for the forward direction.

Third, on time scales of a few run/tumble events, the dynamics is described by the effective equation

$$\partial_t n + \nabla\cdot(\chi n\nabla c) = \nabla^2[D_0(1+\gamma c)n] \quad [5]$$

for the probability density $n(\boldsymbol{x},t) \equiv \int P(\boldsymbol{x},t,\hat{\boldsymbol{u}},\boldsymbol{m})d\hat{\boldsymbol{u}}d\boldsymbol{m}$ of the bacterium space-time position. Eq. **5** is derived from the Fokker–Planck Eq. **4** by homogenization methods akin to those of multiscale models in refs. 31 and 32. In deriving Eq. **5**, we use that the chemotactic modulation is weak, which was already the assumption in Eq. **1**. Because diffusion without any chemoattractant is isotropic, weak modulation implies small departures from isotropy. Eq. **5** is local, despite the correlations generated by bacterial runs, because it describes the dynamics only at scales larger than those correlations, in analogy with hydrodynamic equations in statistical physics.

Two terms in Eq. **5** are quite familiar: The Laplacian $D_0\nabla^2 n$ describes the bacterial diffusion in space, and the term proportional to χ accounts for the drift in response to spatial gradients ∇c of chemoattractant. The bacterial diffusivity reads $D_0 = u^2/3\sigma$, and the chemotactic drift coefficient $\chi = 2D_0(3\sigma\tau_r)^{-1}\int_0^\infty e^{-\sigma t}K(t)dt$ (these expressions are the special case $d = 3$ of the general d-dimensional formulas derived in *SI Text*), where $\sigma = (6D\tau_r + 2)/3\tau_r$ and we recall that D is the rotational diffusivity. The term proportional to γ in Eq. **5** is physically interpreted as a concentration-dependent modification of the bacterial diffusivity. This effect plays a fundamental role in what follows because $\gamma = 2(3\sigma\tau_r)^{-1}\int_0^\infty K(t)dt$ is proportional to the integral of the response.

The fourth and final step is to consider small concentrations of chemoattractant and treat perturbatively chemotactic terms in Eq. **5**. The quantity of interest is the uptake of chemoattractant defined as

$$S \equiv \int dxdtc(\boldsymbol{x},t)n(\boldsymbol{x},t). \quad [6]$$

The fields $c(\boldsymbol{x},t)$ of interest for the maximin strategy in the next section will turn out to decay rapidly in time so that the integral in Eq. **6** converges. The uptake is a quantitative measure of the amount of chemical intercepted by the bacterium along its trajectory. The notion of uptake should not be understood as implying that the chemical is necessarily metabolized by the bacterium: It is known indeed that a few chemoattractants are just a proxy that bacteria track but do not directly consume (5). By expanding Eq. **5** at the lowest order, all the terms involving c are neglected and only diffusion with coefficient D_0 is left. In the next-leading contribution, modulation due to chemotaxis appears; the corresponding solution is expressed in terms of the Gaussian diffusion propagator $G(\boldsymbol{x},t) = (4\pi D_0 t)^{-d/2}\exp[-\boldsymbol{x}^2/(4D_0 t)]$. The resulting expression $S = S_0 + S'$ for the uptake in Eq. **6** yields

$$S_0 = \int dsd\boldsymbol{x}G(\boldsymbol{x},s)c(\boldsymbol{x},s); \qquad S' = \chi a[c] + D_0\gamma b[c]. \quad [7]$$

The component S_0 is the chemoattractant intercepted in the absence of chemotaxis, whereas S' is the additional (or depleted) amount due to the chemotactic modulation. The uptake S_0 depends on the bacterial diffusivity D_0, which depends itself on the running time τ_r. The profile $c(\boldsymbol{x},t)$ affects the uptake S' via the two coefficients

$$a[c] = \frac{1}{2}\left\langle\left[\int_0^\infty ds\nabla c(\boldsymbol{X}_s,s)\right]^2\right\rangle_{W_t}, \quad [8]$$

$$b[c] = \left\langle\int_0^\infty ds\int_0^s ds'c(\boldsymbol{X}_{s'},s')\nabla^2 c(\boldsymbol{X}_s,s)\right\rangle_{W_t}. \quad [9]$$

The angle brackets denote the average over the paths $\boldsymbol{X}_t$ that obey $d\boldsymbol{X}_t = \sqrt{2D_0}\boldsymbol{W}_t$, where $\boldsymbol{W}_t$ is the d-dimensional Wiener process. In other words, $\boldsymbol{X}_t$ is the diffusive trajectory followed by the bacterium in the absence of chemoattractant. The coefficient $a[c]$ is nonnegative and vanishes for spatially uniform profiles. Moreover, by standard inequalities, if $|c|$ and $|\nabla^2 c|$ are bounded, so are a and $|b|$. Finally, the bacterium diffusivity D_0 enters Eqs. **8** and **9** via the statistics of the diffusing trajectories involved in the averaging over W_t.

Maximizing the Minimum Bacterial Uptake (Maximin)

Equations **7–9** express the chemotactic contribution to the bacterial uptake as a quadratic form of the chemoattractant profile

$c(\boldsymbol{x},t)$. The kernel of the quadratic form carries the information on the bacterial parameters, i.e., response function $K(t)$ and running time τ_r. For each choice of these parameters, the kernel of the form has a minimal eigenvalue and eigenvector, i.e., a chemoattractant profile that gives the minimum uptake for those bacterial parameters $K(t)$ and τ_r. As we detail in *SI Text*, the calculation of the minimal eigenvalues is feasible analytically. Indeed, by taking the Mellin transform in time and expanding over associated Laguerre polynomials in the space variable, the kernel of the uptake quadratic form is reduced to a form diagonal in the Mellin variable s and tridiagonal in the indices of the Laguerre polynomials. Furthermore, the tridiagonal reduces to diagonal for $\gamma = 0$, with the first diagonal element (and lowest eigenvalue) equal to zero and all the other elements increasing along the diagonal and positive. For small γs, the tridiagonal form of the matrix yields the analytical expression of the lowest eigenvalue $\propto -D_0\gamma^2/\chi$. We conclude that the lowest eigenvalue has a local maximum at $\gamma = 0$, and it is checked numerically that the maximum is global. The conclusion is valid for all Mellin variables s; i.e., no particular restriction applies to the field $c(\boldsymbol{x},t)$. A chemotactic response $K(t)$ with zero integral $\gamma = 0$ thus emerges naturally as the optimality condition of largest minimum uptake (maximin strategy).

Whereas detailed calculations are reserved to *SI Text*, the reasons why the maximin strategy naturally yields responses $K(t)$ with zero integral can be understood from Fig. 2. Chemoattractant profiles that give the minimum bacterial uptake turn out to be rapidly decaying in time, as intuitively expected. A local analysis of the profiles is then sufficient to capture the main qualitative features. Responses $K(t)$ with a negative integral perform poorly in escaping from a minimum of concentration because the effect of negative γ is to reduce the effective diffusivity (see Eq. **5**). Conversely, the increase of the bacterial diffusivity for positive γ is penalized while trying to keep advantageous positions around local maxima of c. The minimal uptake for both previous choices is therefore low. As shown in Fig. 2, the option guaranteeing the largest minimal uptake for the bacterium is $\gamma = 0$. Note that there is nothing intrinsically wrong with $\gamma \neq 0$:

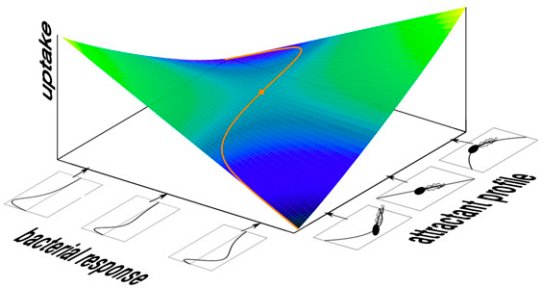

Fig. 2. A pictorial view of the phase space for the chemoattractant bacterial uptake. The bacterial strategies are compactly represented by a single variable, the integral γ of the chemotactic response, at fixed drift coefficient χ and running time τ_r. Three response functions $K(t)$ with positive, zero, and negative γ are shown on the bacterium axis. Chemoattractant profiles are also summarized by a single variable that condenses the information on the local chemoattractant profile around the bacterial location (a relevant proxy is the ratio b/a of the two coefficients appearing in Eqs. **8** and **9**). Responses $K(t)$ with a negative integral perform poorly in escaping from a minimum of chemoattractant concentration, yet they are advantageous in keeping the bacterium localized around a maximum. The opposite holds true for positive γs. Extreme values of γ are thus ensuring high uptakes in some particular conditions, yet they perform poorly in others. The orange line shows the minimum uptake of chemoattractant for each choice of the bacterial response; the maximum among these minima is shown by a circle. The latter gives the response $K(t)$ that guarantees the highest minimal uptake irrespectively of the chemoattractant profile that the bacterium will experience. This maximin strategy yields a chemotactic response $K(t)$ having zero integral $\gamma = 0$, as the experimental one in Fig. 1.

Such choices ensure, in fact, maximal uptakes larger than for $\gamma = 0$ yet in specific ranges of natural conditions. In other words, we are before the chemotactic version of the classical specialist vs. generalist trade-off, with the former favored in particular conditions and the latter emerging as variability and fluctuations increase.

Fig. 2 also shows that the lowest eigenmodes of the uptake quadratic form are largely determined by local properties of $c(\boldsymbol{x},t)$ (level, slopes, and curvatures) around the initial location of the bacterium and that they have rather simple space-time structures (see *SI Text*). Minimal configurations are thus easy to generate in natural conditions, e.g., by the combined effect of environmental inhomogeneities of nutrient patches, the absorption of chemoattractants by other bacteria in a colony, and the smoothing effect of diffusion. In other words, the lowest eigenmodes of the uptake quadratic forms are expected to be generated with nonvanishing likelihood in natural conditions.

The maximin response is the only one that outperforms motile nonchemotactic bacteria (same running time τ_r but $K \equiv 0$ in Eq. **1**) *in all chemoattractant profiles.* Indeed, the eigenmode giving the minimum uptake at $\gamma = 0$ is almost uniform, with small fluctuations that decay rapidly in time. Because in Eq. **8** the coefficient $a[c] \geq 0$, the corresponding uptake is nonnegative and chemotactic responses with $\gamma = 0$ (and chemotactic drift $\chi > 0$) are the only ones that enjoy this property (see *SI Text*).

For $\gamma = 0$, the uptake is maximized by the largest chemotactic coefficient χ. Maximizing the expression of χ (see *SI Text*) at fixed $\gamma = 0$, i.e., $\beta_2 = -\beta_1/2$ in Eq. **2**, finally yields the maximin prediction

$$K(t) = \beta_1 \lambda e^{-\lambda t}[\lambda t - (\lambda t)^2/2]; \qquad \lambda = \frac{4(1+3D\tau_r)}{3\tau_r}; \qquad \tau_r = \frac{1}{3D}; \qquad \textbf{[10]}$$

where we recall that D is the rotational diffusivity and the overall amplitude β_1 is a free parameter (see *SI Text* for nonlinear effects). The comparison between Eq. **10** and the experimental data (18) is excellent, as shown in Fig. 1. Eq. **10** agrees with the intuition that relevant time scales are set by rotational diffusion (28). Indeed, larger D induce shorter run durations τ_r and a faster decay of the response $K(t)$, i.e., shorter memory. The memory time $\lambda\tau_r = 8/3$ is a fraction of the running time, as expected. Including higher-order terms in the expansion [**2**] yields curves very similar to Eq. **10**, $\gamma = 0$ is unchanged, and only numerical factors relating λ and τ_r to D are slightly modified (see *Higher-Order Parameterization of the Response Function* of *SI Text*). Small corrections to Eq. **10** due to the finite duration of tumblings are computed in *Finite Tumbling Time* of *SI Text*. In *Rotational Diffusivity: Comparison with Experiments* of *SI Text*, we also show that values of the rotational diffusivity D obtained from the maximin relation are compatible with data on the angular deviations observed in the direct tracking of bacteria (6).

Relations to Game Theory

Maximin strategies are known in game theory (and its diverse applications to economy, finance, behavioral psychology, etc.) as the extreme risk-aversion choice of actions (see, e.g., refs. 33 and 34). Considering zero-sum games with two players (where the amount won by player I corresponds to the loss of its opponent, player II), the maximin strategy ensures a gain known as the floor (lower) value of the game. This value is the gain of player I guaranteed even when its strategy is disclosed to its opponent, i.e., in the most hostile and favorable conditions for player I and II, respectively. The inverted situation and the corresponding strategy is known in game theory as the minimax strategy, which gives the so-called ceiling (upper) value of the game (33, 34). In other words, it is now the opponents' strategy that gets disclosed and player I can capitalize on this privilege.

Our problem can be formulated as a game by introducing an opponent player (dubbed "nature") to the individual bacterium. The opponent represents all the actors shaping the statistics of the chemoattractant fields $c(\boldsymbol{x},t)$ experienced by the individual bacterium. These actors include both the environment and the rest of the colony that surrounds the bacterium. As explained in the Introduction, environmental conditions where chemotaxis is selected are hostile and bacteria in the colony vie for a limited amount of resources. Chemoattractants are therefore expected to be scarce and actively deformed by the colony. This competitive action of the colony on the chemoattractant field $c(\boldsymbol{x},t)$ is what should be understood as the "strategy of nature." The individual bacterium opposes to the strategy of nature its own strategy, which consists of the choice of the chemotactic response $K(t)$ and running time τ_r. The conflicting goal of the strategies of nature and the individual bacterium is maximizing their respective uptake of chemoattractant. The zero-sum condition on the game is natural to interpret when the chemoattractant is consumed by bacteria, because the amount taken up by one bacterium will not be available for the rest of the colony (and vice versa).

Minimax strategies can now be formulated for the chemotactic game against nature. The upper value of the game is obtained in the following situation: "Nature" can shape an arbitrary chemoattractant profile, yet the profile is "known" to the individual bacterium, which adapts its response to that particular field. These conditions are analogous to those considered in refs. 21 and 22 (where the bacterial uptake was maximized for a given chemotactic profile), and *Best Bacterial Response to Given Chemoattractant Profiles (Minimax)* of *SI Text* shows indeed that minimax responses are single-lobe, as in refs. 21 and 22. The distinction mentioned in the Introduction between regular vs. irregular environments appears then to relate to the game-theoretical differences between minimax vs. maximin. In the former case, the strategy of nature is known to the bacterium in the sense that environmental conditions are stable enough to be "learned" in the evolution of the response. Conversely, for complex fluctuations of the environment, the bacterium should expect to face with its strategy of response *any* possible natural condition. Experiments (25–27) and the agreement in Fig. 1 indicate that the maximin strategy is the one relevant to bacterial chemotaxis. The asymmetry between the two players in the maximin strategy is intuitive, because if an individual bacterium's strategy outperforms the others, it will invade the colony and will then be known by its clones that populate the colony.

MaxiMin Strategy from Evolution in a Chemostat

This section will demonstrate the emergence of the maximin strategy from Darwinian selection, under mild conditions on the relation between fitness (increase in biomass) and chemoattractant uptake.

The *E. coli* life cycle alternates between nutrient-rich phases in the human body and periods spent in the environment. Flagella are not lost in humans probably because motility is useful for reasons other than chemotaxis. One notable possibility is aerotaxis, because *E. coli* comprise about 0.3% of the bacteria in the gut and the vast majority of other microorganisms are strictly anaerobic, so that the *E. coli* niche should be at the periphery, where oxygen is available. The sense from experiments (25–27) is that chemotaxis is under selection in the phase outside of the human body, where nutrients (and cues to locate them) are scarce. The resulting qualitative picture is that nutrient-rich phases alternate with bottlenecks where chemotaxis is crucial for chasing patches of nutrients needed for survival.

The population dynamics during bottlenecks is conveniently analyzed by considering a chemostat in the regime of low nutrient influx. In Fig. 3 we show the results of numerical simulations of bacteria endowed with different chemotactic responses to a chemoattractant, which we suppose for simplicity to be also a limiting nutrient consumed by the bacteria. The average density of each bacterial species evolves according to Monod's equation, whereas the average nutrient concentration results from the balance between inflow and consumption. At variance with classical models of the chemostat (see ref. 35), we consider explicitly the presence of random space-time fluctuations due to the localized absorption by individual bacteria. These fluctuations are characterized by a typical time scale of a few seconds, which is set by the bacterial uptake. The correlation length scale results from the balance between nutrient diffusion and uptake and is of the order of a few tens of microns. In the harsh low-dilution regime, the active absorption by bacteria makes concentration fields that are characterized by a large number of local minima and maxima that vary rapidly in time. The major source of variability in the uptake is the local "curvature" term $b[c]$ in Eq. **9**. The dependency between growth and uptake rates is assumed to have a Michaelis–Menten form [derived systematically in Droop's model (35)]. The actual form is not determinant, as long as the growth rate is an increasing, concave function of the uptake rate. The latter property is key in penalizing wide fluctuations in the uptake typical of chemotactic responses with nonzero γs (see Fig. 3).

Let us indeed consider two situations characterized by the same average uptake but different widths of its fluctuations. By Jensen's inequality, the concavity of the relation between growth rate and uptake makes the average growth rate higher for the situation where fluctuations are more reduced. Fig. 3 and the arguments presented in *SI Text* show that different response functions lead indeed to a competition as that just described. Because responses with $\gamma = 0$ have the smallest fluctuations, they finally invade the bacterial population (see Fig. 3).

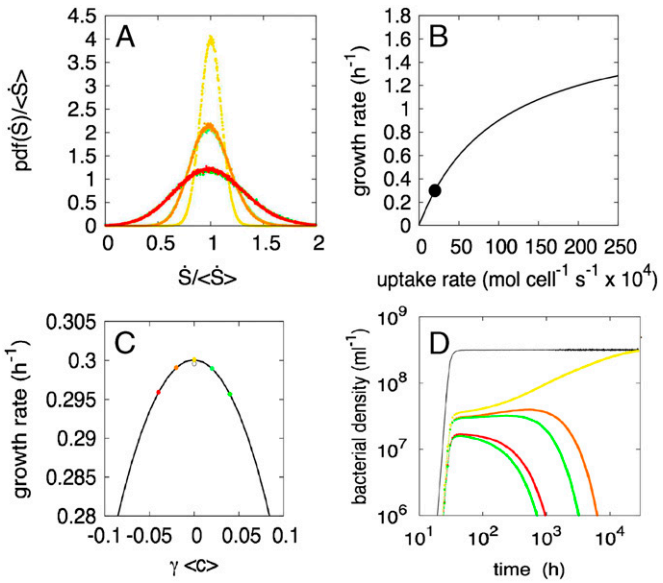

Fig. 3. Competitive exclusion in the chemostat. The nutrient concentration has a mean value $\langle c\rangle \simeq 1$ μM. Fluctuations have an intensity of 10% with respect to the mean, correlation length 40 μm, and correlation time 5 s. The color coding is red for $\gamma\langle c\rangle = -0.04$, orange for $\gamma\langle c\rangle = -0.02$, yellow for $\gamma = 0$, and light and bright green for $\gamma\langle c\rangle = 0.02$ and $\gamma\langle c\rangle = 0.04$, respectively. Other parameters are $D_0 = 400$ μm^2/s and $\chi\langle c\rangle = 40$ μm^2/s. (*A*) The probability density function of the uptake rate $\dot{S}$ ($\langle\dot{S}\rangle = 2\cdot 10^5$ molecules/cell s). Note that the excursions increase with γ and that the probability density functions are nearly identical for γ and $-\gamma$. (*B*) The functional dependence of bacterial growth rate on the uptake rate is $\mu = \mu_{\max}\dot{S}/(\dot{S}+\dot{S}_\star)$, with $\mu_{\max} = 1.8$ h^{-1} and $\dot{S}_\star = 10^6$ molecules/cell s. The full circle marks the point where the growth rate equilibrates the chemostat dilution rate 0.3 h^{-1}. (*C*) Average growth rate $\langle\mu(\dot{S})\rangle$. The curve has a global maximum at $\gamma = 0$. The empty circle (below the yellow one) denotes the growth rate for nonchemotactic bacteria. (*D*) Population dynamics showing that bacteria with $\gamma = 0$ exclude all competitors and reach a final density that equals the total bacterial density (full black line).

Additionally, the effect of concavity increases as the average uptake rate diminishes, so that the harsher the environmental conditions, the more effective is the selection process that makes the maximin strategy emerge.

Conclusions

A consequence of our results is that bacterial chemotaxis appears to be selected in chemoattractant profiles where local gradients vary appreciably in space and time. Strong fluctuations in the gradients justify the need for their effective detection, which goes well with the qualitative standard argument that zero-integral responses are good for sensing. Quantitative points brought here are as follows. First, we considered the effects of the response function's choice upon the amount of chemoattractant intercepted by the bacterium and not separately on sensing and motility performances, which is crucial because the two functions are strongly coupled in *E. coli*. Second, because *E. coli* natural conditions are highly variable, we explicitly considered the dependency on the environment and showed that the experimentally observed response ensures the largest minimum uptake *in any environmental condition* (maximin). Third, the maximin was shown to be the only response that always outperforms motile but nonchemotactic bacteria, justifying chemotaxis as compared to shutting off the signaling pathway and letting the bacterium diffuse randomly. Finally, in the example of the chemostat we showed how the maximin conditions can emerge from Darwinian selection under mild conditions on the relation between uptake and fitness (increase in biomass). Note that the need of strong environmental fluctuations for a zero-integral response also agrees with the remark in ref. 36 that no double-lobe responses emerge from *in silico* evolution in regular and static profiles of chemoattractants.

The generality of our methods makes them applicable to other biological systems. The unique aspect is that optimization is not sought on average but in the most severe environmental conditions. The advantage of the maximin formulation is that it avoids the usual obstacle that the statistics of the environmental fluctuations ought to be known and that the optimal solution will depend on that statistics. The example of the chemostat discussed here illustrates one possibility for the maximin conditions to emerge from Darwinian selection; it will be of interest to analyze the same issue in other situations.

We conclude with a few remarks on the classical observation that clonal colonies feature diversity in their motility (37), which stems from the small number of molecules in the chemotactic pathway (38). As shown in the section on game theory, the dynamics of a whole colony was condensed here into a single adversarial player, similarly to mean-field models in physics, which usually provide only approximate predictions for fluctuations. Yet our results suggest that the diversity in a population should be extremely weak in the integral of the response γ and stronger in the memory λ and the running time τ_r. Indeed, variations in the rotational diffusivity D of individual bacteria are expected at the level of both thermal (6) and mechanical (39) contributions. It is known that the diversity of τ_r is appreciable; it will be of interest to gather experimental data on the correlations among variations in τ_r and those in D and λ. More generally, experiments aimed at quantifying the diversity of the chemotactic response itself and its evolution in well-controlled environments would be highly valuable. One could, in particular, analyze changes and evolution of the bacterial response in random environments with prescribed statistics. Data will bring additional information and permit us to refine our understanding of the optimization principles at work in shaping biological responses to complex environmental fluctuations.

ACKNOWLEDGMENTS. This work was partially supported by the Centre National de la Recherche Scientifique (Program "Prise de risques interface physique-biologie") and the Agence Nationale de Recherches (Programs PIRIbio and PNANO).

1. Wolf DM, et al. (2008) Memory in microbes: Quantifying history-dependent behavior in a bacterium. *PLoS One*, 3:e1700.
2. Mitchell A, et al. (2009) Adaptive prediction of environmental changes by microorganisms. *Nature*, 460:220–224.
3. Kussell E, Leibler S (2005) Phenotypic diversity, population growth, and information in fluctuating environments. *Science*, 309:2075–2078.
4. Acar M, Mettetal JT, van Oudenaarden A (2008) Stochastic switching as a survival strategy in fluctuating environments. *Nat Genet*, 40:471–475.
5. Berg HC (2003) *E. coli in Motion* (Springer–Verlag, New York).
6. Berg HC, Brown DA (1972) Chemotaxis in Escherichia coli analysed by three-dimensional tracking. *Nature*, 239:500–504.
7. Turner L, Ryu WS, Berg HC (2000) Real-time imaging of fluorescent flagellar filaments. *J Bacteriol*, 182:2793–2801.
8. Eisenbach M (2004) *Chemotaxis* (Imperial College Press, London).
9. Barkai N, Leibler S (1997) Robustness in simple biochemical networks. *Nature*, 387:913–917.
10. Alon U, Barkai N, Surette MG, Leibler S (1999) Adaptation in bacterial chemotaxis. *Nature*, 397:168–171.
11. Duke TAJ, Bray D (1999) Heightened sensitivity of a lattice of membrane receptors. *Proc Natl Acad Sci USA*, 96:10104–10108.
12. Kollmann M, Lovdok L, Bartholomé K, Timmer J, Sourjik V (2005) Design principles of a bacterial signalling network. *Nature*, 438:504–507.
13. Mello BA, Tu YH (2005) An allosteric model for heterogeneous receptor complexes: Understanding bacterial chemotaxis responses to multiple stimuli. *Proc Natl Acad Sci USA*, 48:17354–17359.
14. Endres RG, Wingreen NS (2006) Precise adaptation in bacterial chemotaxis through assistance neighborhoods. *Proc Natl Acad Sci USA*, 103:13040–13044.
15. Keymer JE, Endres RG, Skoge M, Meir Y, Wingreen NS (2006) Chemosensing in Escherichia coli: Two regimes of two-state receptors. *Proc Natl Acad Sci USA*, 103:1786–1791.
16. Emonet T, Cluzel P (2008) Relationship between cellular response and behavioral variability in bacterial chemotaxis. *Proc Natl Acad Sci USA*, 105:3304–3309.
17. Bray D, Levin MD, Lipkow K (2007) The chemotactic behavior of computer-based surrogate bacteria. *Curr Biol*, 17:12–19.
18. Segall JE, Block SM, Berg HC (1986) Temporal comparisons in bacterial chemotaxis. *Proc Natl Acad Sci USA*, 83:8987–8991.
19. Silverman M, Simon M (1974) Flagellar rotation and mechanism of bacterial motility. *Nature*, 249:73–74.
20. Strong SP, Freedman B, Bialek W, Koberle R Adaptation and optimal chemotactic strategy for E. coli. *Phys Rev E*, 57:4604–4617.
21. de Gennes PG (2004) Chemotaxis and the role of internal delays. *Eur Biophys J*, 33:691–693.
22. Clark DA, Grant LC (2005) The bacterial chemotactic response reflects a compromise between transient and steady-state behavior. *Proc Natl Acad Sci USA*, 102:9150–9155.
23. Kafri Y, da Silveira RA (2008) Steady-state chemotactic response in E. coli. *Phys Rev Lett*, 100:238101.
24. Vlamakis H, Aguilar C, Losick R, Kolter R (2008) Control of cell fate by the formation of an architecturally complex bacterial community. *Genes Dev*, 22:945–953.
25. Adler J, Templeton B (1967) The effect of environmental conditions on the motility of Escherichia coli. *J Gen Microbiol*, 46:175–184.
26. Amsler CD, Cho M, Matsumura P (1993) Multiple factors underlying the maximum motility of Escherichia coli as cultures enter post-exponential growth. *J Bacteriol*, 175:6238–6244.
27. Staropoli JF, Alon U (2000) Computerized analysis of chemotaxis at different stages of bacterial growth. *Biophys J*, 78:513–519.
28. Berg HC, Purcell EM (1977) Physics of chemoreception. *Biophys J*, 20:193–219.
29. Paster E, Ryu WS (2008) The thermal impulse response of Escherichia coli. *Proc Natl Acad Sci USA*, 105:5373–5377.
30. Tu Y, Shimizu TS, Berg HC (2008) Modeling the chemotactic response of Escherichia coli to time-varying stimuli. *Proc Natl Acad Sci USA*, 105:14855–14860.
31. Erban R, Othmer H (2004) From individual to collective behavior in bacterial chemotaxis. *SIAM J Appl Math*, 65:361–391.
32. Xue C, Othmer H (2009) Multiscale models of taxis-driven patterning in bacterial populations. *SIAM J Appl Math*, 70:133–167.
33. von Neumann J, Morgenstern O (1944) *Theory of Games and Economic Behavior* (Princeton Univ Press, Princeton).
34. Owen G (1995) *Game Theory* (Academic, New York).
35. Smith HL, Waltman P (1995) *The Theory of the Chemostat: Dynamics of Microbial Competition*, Cambridge Studies in Mathematical Biology (Cambridge Univ Press, Cambridge, UK), Vol 13.
36. Goldstein RA, Soyer OS (2008) Evolution of taxis responses in virtual bacteria: Non-adaptive dynamics. *PloS Comput Biol*, 4:e1000084.
37. Spudich JL, Koshland DE Jr (1976) Non-genetic individuality: Chance in the single cell. *Nature*, 262:467–471.
38. Levin MD, Morton-Firth CJ, Abouhamad WN, Bourret RB, Bray D (1998) Origins of individual swimming behavior in bacteria. *Biophys J*, 74:175–181.
39. Locsei JT, Pedley TJ (2009) Bacterial tracking of motile algae assisted by algal cell's vorticity field. *Microb Ecol*, 58:63–74.